Effects of solute breakthrough curve tail truncation on residence time estimates: A synthesis of solute tracer injection studies

J. D. Drummond,[1] T. P. Covino,[2] A. F. Aubeneau,[1] D. Leong,[3] S. Patil,[4] R. Schumer,[5] and A. I. Packman[1]

Received 6 March 2012; revised 21 June 2012; accepted 23 June 2012; published 11 August 2012.

[1] Hydrologic transport and retention strongly affect biogeochemical processes that are critical to stream ecosystems. Tracer injection studies are often used to characterize solute transport and retention in stream reaches, but the range of processes accurately resolved with this approach is not clear. Solute residence time distributions depend on both in-stream mixing and exchange with the hyporheic zone and the larger groundwater system. Observed in-stream breakthrough curves have most commonly been modeled with in-stream advection-dispersion plus an exponential residence time distribution, but process-based models suggest that hyporheic exchange is a fractal process, and that hyporheic residence time distributions are more appropriately characterized by power law tailing. We synthesized results from a variety of tracer-injection studies to investigate the information content of tracer breakthrough curves. We found that breakthrough curve tails are often not well characterized in stream tracer experiments. The two main reasons for this are: 1) experimental truncation of breakthrough curves, which occurs when sampling ends before all tracer mass reaches the sampling location, and 2) sensitivity truncation of breakthrough curves, when tracer concentrations in the tail are too low to be detected reliably above background levels. Tail truncation reduces observed mass recovery and obscures assessment of breakthrough curve tailing and solute residence time. Failure to consider tail truncation leads to underestimation of hyporheic exchange and solute retention and to corresponding overestimation of hyporheic biogeochemical transformation rates. Based on these findings, we propose criteria for improved design of in-stream tracer injection experiments to improve assessment of solute tailing behavior.

Citation: Drummond, J. D., T. P. Covino, A. F. Aubeneau, D. Leong, S. Patil, R. Schumer, and A. I. Packman (2012), Effects of solute breakthrough curve tail truncation on residence time estimates: A synthesis of solute tracer injection studies, *J. Geophys. Res.*, *117*, G00N08, doi:10.1029/2012JG002019.

1. Introduction

[2] Stream tracer-injection studies are often used to estimate solute transport and retention in streams. Regions that slow downstream transport, such as surficial pools or dead zones, and the subsurface hyporheic zone are important to stream biogeochemical processing [*Peterson et al.*, 2001; *Haggerty et al.*, 2002; *Battin et al.*, 2008; *Alexander et al.*, 2009]. Substantial stream metabolic activity and nutrient transformation occurs in stream sediments, where solute residence times are increased and microbial biomass occurs in the form of biofilms [*Triska et al.*, 1989; *Argerich et al.*, 2008]. The strong control of solute residence times in the hyporheic zone on biogeochemical processing rates, specifically net nitrification and denitrification, has been demonstrated with direct measurements [*Zarnetske et al.*, 2011]. However, since most studies do not directly measure solute concentration in storage areas, the residence time of solutes is deduced from main-channel (i.e., thalweg) sampling. Typically, tracers are injected at an upstream location and observed to propagate past one or more downstream sampling locations [*Harvey and Wagner*, 2000]. The concentration-time history of tracer observed at a sampling site downstream is known as the breakthrough curve, and can be fit with a transport model to estimate stream transport parameters such as advection, dispersion, and transient storage [*Fischer et al.*, 1979; *Stream Solute Workshop*, 1990]. The rising limb and peak or plateau portions of the breakthrough curve represent quicker solute transport paths and the tailing limb indicates

[1]Department of Civil and Environmental Engineering, Northwestern University, Evanston, Illinois, USA.
[2]Nicholas School of the Environment, Duke University, Durham, North Carolina, USA.
[3]Department of Geography, University of British Columbia, Vancouver, British Columbia, Canada.
[4]School of Civil and Environmental Engineering, Georgia Institute of Technology, Atlanta, Georgia, USA.
[5]Division of Hydrologic Sciences, Desert Research Institute, Reno, Nevada, USA.

Corresponding author: J. D. Drummond, Department of Civil and Environmental Engineering, Northwestern University, 2145 Sheridan Rd., Evanston, IL 60208, USA. (j-drummond@u.northwestern.edu)

0148-0227/12/2012JG002019

solute transferred into slower transport paths including surface and hyporheic storage zones.

[3] In streams with limited storage areas, such as only surface water storage [*Gooseff et al.*, 2005], a model assuming in-stream advection-dispersion with an exponential residence time distribution of solute in one or more fixed storage areas may be appropriate [*Bencala and Walters*, 1983; *Choi et al.*, 2000]. Alternatively, when a breakthrough curve is highly skewed, indicating a wide range of storage times along the stream reach, model fits are improved by assuming a power law residence time distribution of solute in storage [*Haggerty et al.*, 2002, *Schumer et al.*, 2003, *Gooseff et al.*, 2005]. In fact, recent experiments and models show that hyporheic or significant interfacial exchange induced by geomorphological features exhibits fractal behavior, leading to a power law residence time distribution of solutes in storage [*Haggerty et al.*, 2000; *Cardenas*, 2008]. Model choice can alter estimation and interpretation of stream transport properties. For example, if a solute breakthrough curve with a long tail is fit with an advection-dispersion equation with an exponential residence time distribution (e.g., OTIS) then the estimated hydrologic parameters will not accurately characterize all timescales of transport within storage zones. Models developed to allow for a wider range of residence times include continuous time random walk (CTRW), multirate mass transfer (MRMT), and solute transport in rivers (STIR) models [*Cortis and Berkowitz*, 2005; *Haggerty and Gorelick*, 1995; *Marion et al.*, 2008].

[4] We compared tracer-injection studies across stream systems in order to improve understanding of solute transport and retention characteristics based on tailing behavior. We found that the majority of breakthrough curve tails were truncated, suggesting that commonly used tracer-injection methods often do not yield sufficient information to accurately characterize solute retention in stream reaches. We present a combination of experimental and theoretical results to demonstrate sources of error commonly encountered in tracer breakthrough curves, and determine the conditions that must be met for long-term solute storage to be accurately characterized. Based on these findings we recommend improved design of tracer injection studies to better characterize hyporheic exchange.

2. Synthesis of In-Stream Injection Results

[5] We synthesized the results of 162 tracer-injections performed in 87 streams. The summary data of the 633 breakthrough curves resulting from the tracer injections presented here are included in the auxiliary materials.[1] The extent of the measured breakthrough curve tail can be taken as the ratio between the time elapsed after cessation of tracer input until the last sampling time (t_{MAX}-$t_{PLATEAU}$) and the characteristic in-stream travel time (t_C), taken as the time to peak for a pulse injection and time to half the maximum concentration for a continuous injection. For a pulse injection $t_{PLATEAU}$ is zero. This ratio will be referred to as the truncation time (t_T), where $t_T = (t_{MAX} - t_{PLATEAU})/t_C$. This calculation for both a pulse and continuous injection is shown in Figures 1a and 1b. The distribution of truncation times for each tracer-injection study is reported in Figure 1c. Only 39 studies characterized long-term breakthrough curve tailing behavior, operationally defined as having a tail truncation time (t_T) greater than 20.

[6] Other criteria used to assess the quality of the breakthrough curve for the data sets with minimal truncation were richness of data in the tail (i.e., density of data at long time-scales) and the dynamic range of tracer data, defined as the ratio between the maximum and minimum tracer concentration measured in-stream for each experiment as shown in Figure 1a and 1b. The larger the dynamic range, the greater the ability to measure tracer at longer time-scales in the tail of the breakthrough curve where the in-stream concentrations approach background levels. The dynamic ranges of the studies with long-term breakthrough curve tailing varied from $1.10e^0$ to $2.91e^7$. Dynamic range is dependent on tracer type, analytical methods, and the background concentration and variability of the tracer. The data sets we reviewed included a variety of tracer types including fluorescent dyes (mainly Rhodamine WT), ionic salts (mainly chloride) and radioisotopes (tritium). Tritium and fluorescent dyes have low backgrounds in freshwater streams, which lead to large dynamic ranges (Table 1). However, background chloride concentrations vary greatly, between 34 and 888 μS/cm for the studies within this review.

[7] Breakthrough curve truncation limits the range of solute retention timescales that can be characterized and makes it difficult to determine the form of the storage residence time distribution. From the synthesis of the experimental observations, we identified two main reasons for truncation of data. One cause of truncation was cessation of sampling before tracer concentrations returned to background levels and we term this experimental truncation. 94% of the 633 breakthrough curves analyzed exhibited experimental truncation. The second cause was a lack of sensitivity of the tracer measurements relative to the background concentration. In this case, while in-stream sampling might have extended for a long time, tracer could not be distinguished from background levels in late-time samples on the breakthrough curve tail. We term this sensitivity truncation. In cases of severe sensitivity truncation, there is not enough difference between the tracer concentration and background concentration to observe a tail. The sensitivity limit can result from analytical errors associated with the measurement technique or to temporal variability in the background tracer concentration. Many studies showed both experimental and sensitivity truncation. 92% of the experiments with long sampling times were truncated due to sensitivity limitations. In these cases, extended sampling did not increase characterization of the tail owing to the lack of measurement sensitivity. The truncation time (t_T) shown in Figure 1 is the experimental truncation based on the sampling cut-off time, but in many cases sensitivity limits further truncated the data.

[8] When either experimental or sensitivity truncation occurs, some amount of tracer mass is not measured in the breakthrough curve tail. Lack of adequate characterization of breakthrough curve tails may prevent accurate assessment of solute exchange, retention, and residence times. Inaccurate assessment of solute residence times can cause overestimation of biogeochemical reaction rates. The mass not measured in the tail of the breakthrough curve is also normally assumed to have been consumed by reactions, which leads to further

[1] Auxiliary materials are available in the HTML. doi:10.1029/2012JG002019.

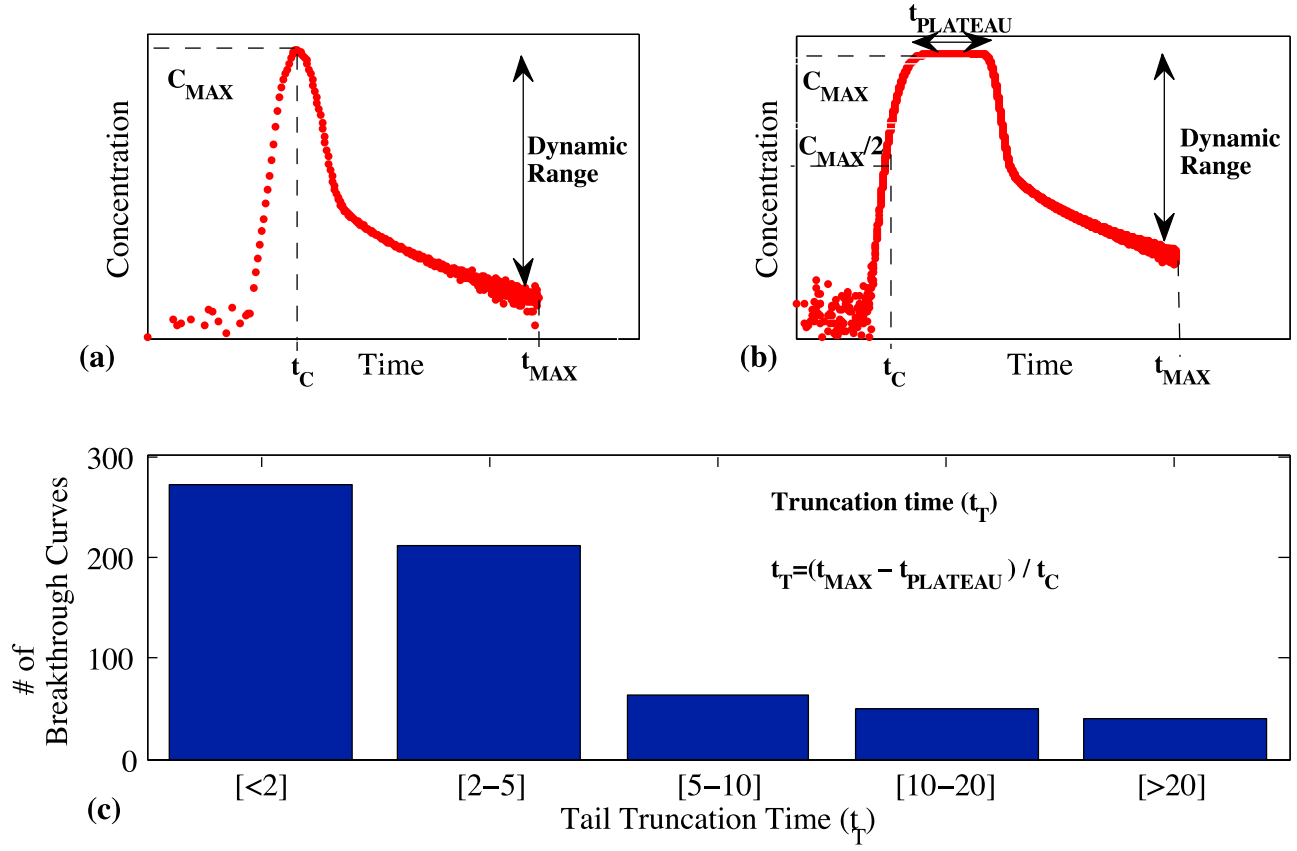

Figure 1. Definition of truncation time (t_T) and dynamic range for a breakthrough curve generated from (a) a pulse or (b) a continuous tracer-injection and (c) distribution of tail truncation times (t_{Ts}) for the 633 experimental breakthrough curves analyzed. The characteristic in-stream travel time (t_C) is the time to peak for a pulse injection and time to half the maximum concentration ($C_{MAX}/2$) for a continuous injection. The last sampling time (t_{MAX}) and the $t_{PLATEAU}$ (zero for a pulse injection) are used to calculate the truncation time (t_T), where $t_T = (t_{MAX} - t_{PLATEAU})/t_C$.

overestimation of reaction rates. We used a combination of experimental results and theoretical analysis to demonstrate the effects of truncation. First we used a breakthrough curve with good characterization of tailing behavior to demonstrate the effects of data truncation. We then used theoretical examples to show the errors that result from truncation of an exactly known solution.

3. Results

3.1. Analysis of In-Stream Injections Showing Long-Term Tailing

[9] In order to investigate the effects of experimental truncation on interpretation of solute storage, we artificially truncated an experimental breakthrough curve with long tailing (t_T = 180.7) generated from a Rhodamine WT pulse injection [*Haggerty et al.*, 2002; *Gooseff et al.*, 2003]. First, we demonstrate the effects of truncation on residence time estimates using moment methods [*McGuire and McDonnell*, 2006; *Luo et al.*, 2006]. The 0th moment represents the mass recovery of tracer in the stream. The first moment (mean) is usually taken as the mean arrival time of solute to the sampling station. The first and second moments are used to calculate the variance that is usually attributed to in-stream dispersion. The experimental breakthrough curve shown in Figure 2a shows variation in tracer background concentrations prior to the propagation of the injection pulse at the sampling station. Following the injection, there is a well-defined peak followed by a power law decay to background values. Although there is an experimental truncation time t_T = 180.7, the tracer concentration becomes statistically indistinguishable with background at approximately t_T = 50. Thus, t_T = 50 is the sensitivity truncation time for this data set. In order to illustrate the effects of truncation, we truncated the breakthrough curve at t_T = 2, 5, 10, 15, 20, 39, 55, 80 and 89, indicated by red boxes in Figure 2a. As shown in Figure 2b, when truncation time increased from t_T = 2 to t_T = 55, the mean arrival time increased from 0.82 to 1.28 h (h) and the variance increased from 0.03 to 4.0 h^2 (h^2). The change in variance is directly related to the in-stream dispersion coefficient, and errors in the estimate of in-stream dispersion will affect the estimate of all other transport parameters. The moments of the data showed scale dependence with sampling time: all the moments of the data increased with increasing t_T and only reached asymptotic values when the tracer concentrations in the breakthrough curve returned to background values. Thus, truncation will

Table 1. Experiments With Observations of Tailing Behavior (Truncation Time (t_T) > 10)

Experiment	Reference	Stream/ID	Date	Discharge ($m^3 s^{-1}$)	Pulse/Continuous	Tracer	Truncation Time (t_T)	Dynamic Range (Cmax/Cmin)
1	*Wörman and Wachniew* [2007]	Hobøl River, Norway/Oct 471m	10/11/2002	0.226	Continuous	Tritium	10.3	4.37E+03
2	*Payn et al.* [2009]	Stinger Creek, MT/7m_2	7/25/2006	0.0224	Pulse	Chloride	12.0	5.27E+00
3	*Gooseff et al.* [2005]	H.J. Andrews Experimental Forest, OR/WSO3_A	4/6/2002	n/a	Continuous	Rhodamine WT	15.8	9.48E+03
4	*Gooseff et al.* [2003]	Lookout Creek, OR/WSO3	4/21/2001	0.026–0.027	Pulse	Rhodamine WT	180.7	2.82E+04

often cause underestimation of the mean travel time, dispersion coefficient, and solute storage time.

[10] Extended multiscale surface-subsurface exchange often produces power law tails in breakthrough curves [*Cardenas*, 2007; *Wörman and Wachniew*, 2007]. In this case, power law decay of a late-time breakthrough curve reflects power law residence times in storage zones. Smaller power law slope or increased tailing reflects storage over a wider range of timescales. We used a continuous time random walk (CTRW) model to fit breakthrough curve data and to analyze the effects of truncation on these slopes. CTRW provides a stochastic description of motion as a sequence of jumps with random length and random duration between initiation of jumps, which allows for general representation of in-stream transport and exchange with storage zones [*Berkowitz et al.*, 2006; *Schumer et al.*, 2003, 2009]. The governing equation for solute transport in streams is [*Boano et al.*, 2007]:

$$\frac{\partial C(x,t)}{\partial t} = \int_0^t M(t-t')\left[-U_\psi \frac{\partial C(x,t')}{\partial x} + K_\psi \frac{\partial^2 C(x,t')}{\partial x^2}\right] dt' \quad (1)$$

where C is in-stream solute concentration, t is the elapsed time, and Uψ and Kψ are the velocity and dispersion coefficients calculated from the moments of the jump length probability density function. This formulation is analogous to the advection-dispersion equation plus a convolution integral with a memory function, M(t), that depends on the exchange flux (Λ) and storage residence time distribution (φ(t)). At any time the memory function represents the mass of solute that has entered a storage area at time t and is still in storage at a later time (t + dt). Multiple storage zones can be represented by associated exchange flux terms (Λ(i)) and storage residence time distributions (φ_i), where i represents each storage zone. We take i = 1 as surface storage and i = 2 as hyporheic storage. Thus, solute storage in both the surface and hyporheic is incorporated into equation (1) through the memory function, M(t). We fit the model to the experimentally observed breakthrough curve using a modified form of the CTRW toolbox, implemented in MATLAB [*Cortis and Berkowitz*, 2005]. (For further details, see S. H. Stonedahl et al., Physical controls and predictability of stream hyporheic flow evaluated with a multiscale model, submitted to *Water Resources Research*, 2012.) Since the data clearly demonstrates power law tailing, we used a power law hyporheic storage residence time distribution ((φ_2),, and analyzed the slope of the power law tail as a representation of hyporheic storage characterization. The optimal fit for this data was to not include surface storage by setting the exchange flux of solute into surface storage to zero (Λ(1) = 0). Although we used the CTRW model framework here, other similar models such as the multirate mass transfer model (MRMT) or solute transport in rivers model (STIR) would yield essentially equivalent results [*Haggerty and Gorelick*, 1995; *Marion et al.*, 2008].

[11] As the tail was truncated from t_T = 55 to t_T = 2, the tail slope increased from 1.34 to 1.74, with an asymptote to the minimum slope value around t_T = 20. As the slope increases, the model attributes less solute storage to the hyporheic region. At a truncation time of 20, the model was able to appropriately characterize solute transport in the stream, as shown by the asymptotic power law slope

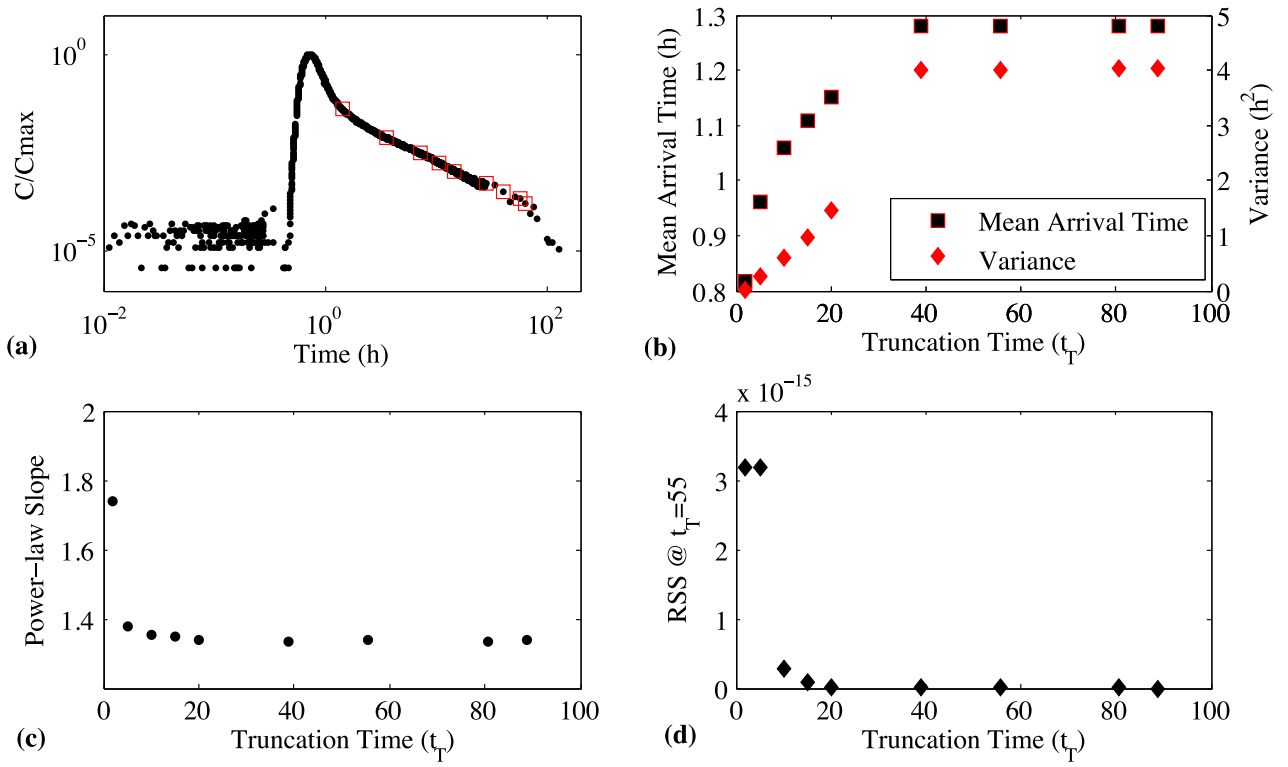

Figure 2. The effects of tail truncation on solute residence time for an experimental breakthrough curve [*Haggerty et al.*, 2002, *Gooseff et al.*, 2003]. (a) The breakthrough curve was truncated at times $t_T = 2$ to $t_T = 89$. (b) Mean arrival time (first moment) and variance for each truncation time. (c) Power law slope of breakthrough curve tail and (d) residual sum of squares (RSS) between the truncated and full data set concentration values at $t_T = 89$ for each truncation time.

(Figure 2c). We demonstrated the error associated with truncation by computing the residual sum of squares (RSS) error between the truncated and full data set model output concentration value at $t_T = 55$ as the tail was truncated. The RSS error increased from 0 to $5.22e^{-14}$ as the tail was truncated from $t_T = 55$ to $t_T = 2$ (Figure 2d). The samples collected at later times extend the tail of the breakthrough curve, provide more accurate characterization of breakthrough curve tailing, and better constrain solute transport and storage metrics. At $t_T < 20$, the storage parameters and solute residence time in the stream were both underestimated. It is important to note that we did not need to extend the tail until background concentrations were reached in order to distinguish the form of the residence time distribution (i.e., power law in this case) and get a good estimate of the asymptotic tail slope.

[12] In many cases the appropriate model and associated residence time distribution must be chosen based on limited data (i.e., truncated tail). As storage and exchange processes are inferred from fitting, it is problematic if alternative residence time distributions (exponential, power law tailing, etc.) cannot be adequately vetted to determine optimal model fits to the data. To demonstrate, we fit two different forms of residence time distributions to an experimentally truncated breakthrough curve ($t_T = 5.8$) obtained from a tritium tracer injection [*Johansson et al.*, 2001] (Figure 3). We fit the data with the following three cases using the CTRW model: one exponential storage zone residence time distribution, two exponential storage zone residence time distributions, and one exponential and one power law storage zone residence time distribution. In each case, the first storage zone residence time distribution is attributed to retention in the surface, while the second represents solute transport and retention in the hyporheic zone. The stream length (L) and injection duration

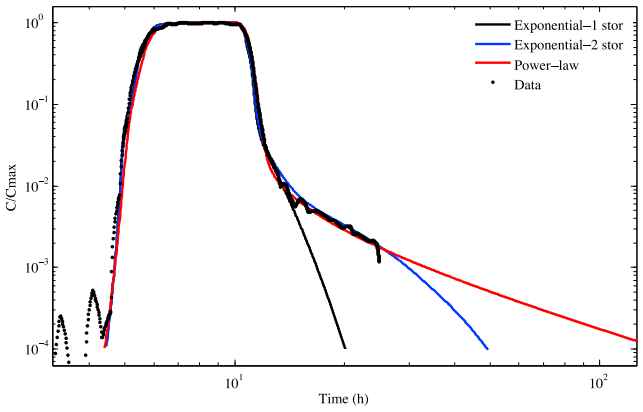

Figure 3. Experimental observations of a tritium breakthrough curve [*Johansson et al.*, 2001] with $t_T = 5.8$ fit to exponential (one storage zone), exponential (two storage zones) and exponential/power law (two storage zones) residence time distributions. The system was simulated using L = 2100 m and an injection duration of 316 min. The optimized velocity, dispersion, and storage parameters are shown in Table 2.

Table 2. Continuous Time Random Walk Model Storage Parameters and Least-Square Fit of Error for the Three Alternative Model Fits Shown in Figure 4

	RSS	Velocity (u) [m s^{-1}]	Dispersion (D) [m s^{-2}]	Flux-1 (Λ_1) [s^{-1}]	Residence Time-1 (Φ_1) [s]	Flux-2 (Λ_2) [s^{-1}]	Residence Time-2 (Φ_2) [s]
Single exponential storage	27.7	$4.98e^{-5}$	$9.14e^{-8}$	$3.32e^{-6}$	$\exp^{-\frac{1}{4954}t}$	N/A	N/A
Double exponential storage	12.1	$4.94e^{-5}$	$9.44e^{-8}$	$2.96e^{-6}$	$\exp^{-\frac{1}{3966}t}$	$1.02e^{-6}$	$\exp^{-\frac{1}{507}t}$
Exponential and power law storage	11.9	$4.95e^{-5}$	$9.15e^{-8}$	$4.97e^{-5}$	$\exp^{-\frac{1}{507}t}$	$4.83e^{-5}$	$t^{-1.35}$

were held constant, while the velocity (u), dispersion (D), flux into (Λ_1 and Λ_2) and residence time distribution within (φ_1 and φ_2) each storage area was selected to minimize the RSS between the data and CTRW model. For all cases L = 2100 m, and the injection duration was 316 min as specified by [*Johansson et al.*, 2001]. The optimized storage parameters and RSS for each model fit are shown in Table 2. The RSS for the single exponential storage model, 27.7, was much larger than the double exponential storage and exponential/power law storage models, which had RSSs of 12.1 and 11.9 respectively. At a truncation of t_T = 5.8 the double exponential and exponential/power law storage models, showed similar RSS values, but based on the experimental case with long tailing behavior previously reviewed, the slope of the power law is not expected to asymptote until a truncation time of $t_T \approx = 20$. Therefore, the RSSs between the double exponential and exponential/power law models is expected to increase as the tail is extended and the power law slope decreases to the asymptotic value. Conversely, the RSSs for the double exponential and exponential/power law models are expected to be closer and the fits will become indistinguishable when the tail is highly truncated. The flux into both the first and second storage zones is greater for the exponential/power law model compared to the double exponential model (Table 2). The double exponential model attributes more retention to surface storage, while the exponential/power law model has similar flux into both the in-stream and hyporheic storage zones. Therefore, the alternative models yield greatly different estimates of solute flux and mean residence time in storage (Table 2).

[13] The *Johansson et al.* experiment also had supporting observations of tracer concentrations in the bed for 100 h past the injection [*Wörman et al.*, 2002]. Figure 4 shows power law and exponential fits to the observed subsurface tritium concentration averaged over depths of 8.5 to 17 cm. The subsurface tracer concentrations are best fit using a power law residence time distribution with a power law slope of 0.98. Further, the asymptotic value of the power law slope of the subsurface residence time distribution is equal to the power law slope of the in-stream breakthrough curve minus 1 [*Schumer et al.*, 2003]. This demonstrates that the proper forms of both the residence time distribution and breakthrough curve in this stream are power laws even though the power law could not be uniquely determined from the best fit of the observed (highly truncated) in-stream breakthrough curve. More generally, transport and storage will not be characterized well from in-stream data that is highly truncated by limited sampling time or poor resolution of the breakthrough curve tail (i.e., experimental or sensitivity truncation). For the *Johansson et al.* data set considered here, the choice of residence time distribution form strongly influenced the results obtained when fitting the breakthrough curve and changed the interpretation of the system behavior. In order to contain enough information to infer hyporheic exchange, the surface breakthrough curve must be extended to clearly allow fitting of the hyporheic signal or be supported by direct subsurface observations.

3.2. Analysis of a Theoretical Case

[14] We used the CTRW model to generate commonly observed forms of tracer breakthrough curves to analyze the effects of truncation without the noise and background variability inherent in experimental data (Figure 5). Breakthrough curves for a double exponential residence time distribution and two different exponential/power law residence time distributions are shown in Figure 5a. The power law cases have different power law slopes representing hyporheic storage, but the same exponential residence time distributions representing surface storage. The mean in-stream velocity and dispersion coefficient were kept constant at 0.104 m s^{-1} and 0.45 m s^{-2}. The breakthrough curve with two exponential storage areas was generated with fluxes $\Lambda_1 = 3e^{-6}$, $\Lambda_2 = 1e^{-6}$ and storage residence time distributions $\varphi_1 = \exp^{-\frac{1}{4000}t}$, $\varphi_2 = \exp^{-\frac{1}{3e4}t}$. The breakthrough curves with exponential/power law residence time distributions had an exponential surface storage with $\Lambda_1 = 5e^{-5}$, $\varphi_1 = \exp -\frac{1}{500}t$ and power law hyporheic storage with $\varphi_1 = \exp -\frac{1}{500}t$, $\Lambda_2 = 5e^{-5}$ and $\varphi_2 = t^{-1.5}$ or $t^{-1.33}$. A breakthrough curve with the same in-stream velocity and dispersion coefficient, but no storage is also shown for comparison. The asymptotic power law slopes (1.5 and 1.33) were chosen to

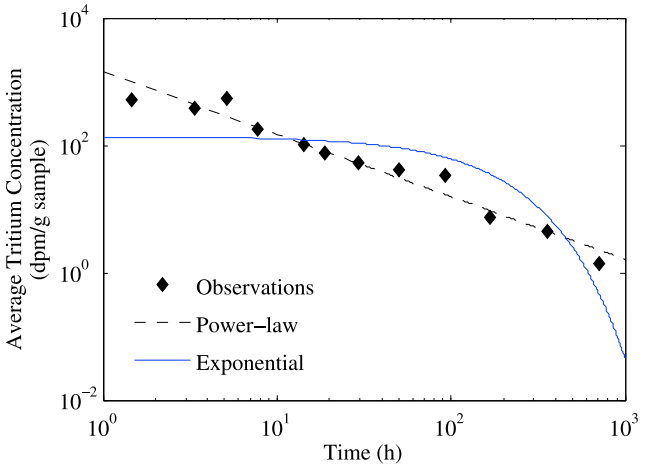

Figure 4. Tritium concentrations observed following in-stream tracer injection in the streambed averaged over sediment depths of 8.5 to 17 cm [*Johansson et al.*, 2001] with a power law ($y = 1429.3 \times^{-0.98}$, $R^2 = 0.96$) and exponential ($y = 136.24e^{-0.008x}$, $R^2 = 0.73$) fit.

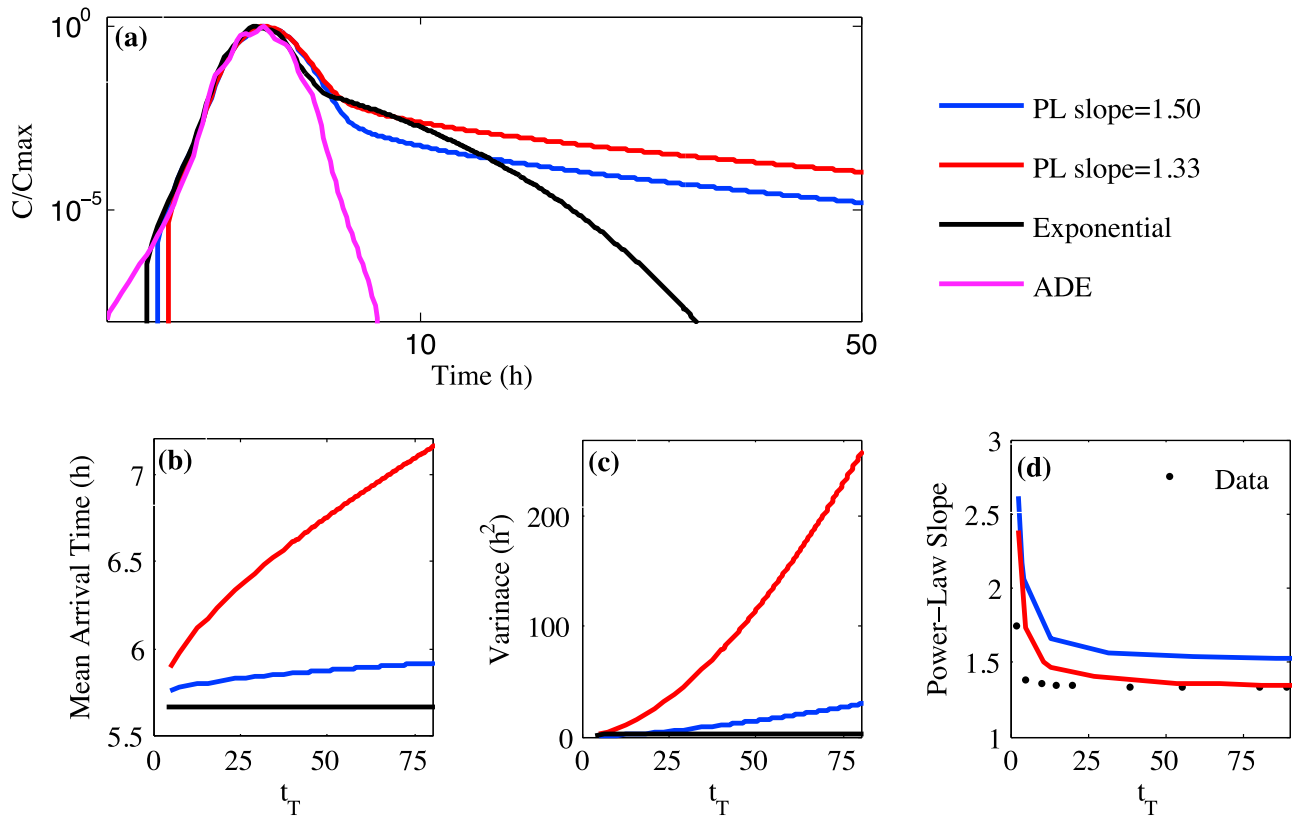

Figure 5. (a) Simulated breakthrough curves of solute breakthrough curves based on exponential and power law (PL) residence time distributions. (b, c, d) Moments and power law slopes calculated for breakthrough curves truncated at varying times (t_T = 2 to t_T = 80). The parameters used were u = 0.104 m s^{-1}, D = 0.45 m s^{-2}, $\Lambda_2 = 5e^{-5}$ and $\varphi_2 = \exp^{-\frac{1}{5000}t}$ for exponential, and $\Lambda_1 = 5e^{-5}$, $\varphi_1 = \exp^{-\frac{1}{500}t}$, $\Lambda_2 = 5e^{-5}$ and $\varphi_2 = t - 1.5$ or t = −1.33 for power law. The ADE simulation does not incorporate any storage.

demonstrate the differences in breakthrough curve behavior even with a slight variation in slope values and are similar to the slopes of the experimental breakthrough curve examples previously presented. Theoretical analysis of solute injections through varying geomorphic features produced power law slopes between 1.6 and 1.9 [*Cardenas*, 2008]. Each breakthrough curve was truncated following the same procedure as the experimental data (Figure 2a) and the moments were calculated at various truncation times ranging from t_T = 2 to t_T = 80 (Figure 5b and 5c). The moments varied greatly depending on the storage residence time distribution used to generate the breakthrough curve. The breakthrough curve resulting from the exponential distribution showed no variation in the moments as the tail was extended because this distribution does not incorporate long-time solute retention. This case yielded a mean arrival time of 5.7 h and a variance of 3.1 h^2 at t_T = 80. The moments of breakthrough curves generated with power law residence time distributions were much greater. Both power law distributions demonstrated scale-dependency in both mean arrival time and variance: the moments continued to increase as the tail was extended and did not reach an asymptotic final value. For the breakthrough curve with power law slope 1.33 the mean arrival time and variance increased from 5.9 h and 1.7 h^2 at t_T = 4 to 7.2 h and 257.4 h^2 at t_T = 80. This is a different result than obtained with the experimental breakthrough curve where the moments reached an asymptote when there was sensitivity truncation associated with reaching the noise level associated with variability in background tracer concentrations. As expected, we observed that increasing the power law slope of the breakthrough curve from 1.33 to 1.5 decreased the moments, indicating less solute retention. At a tail truncation time of 80, the first moments were 7.2 h and 5.9 h for power law slopes of 1.33 and 1.5, respectively. This demonstrates that it is important to obtain good estimates of asymptotic breakthrough curve power law slopes in order to appropriately estimate hyporheic solute residence times. Although the moments of the power law distributions continued to increase as the tail was extended, the power law slope converged to an asymptotic value at $t_T \approx$ = 20 (Figure 5d). This indicates that sufficient stream characterization can be achieved in a truncation timeframe of t_T = 20. As demonstrated with both experimental and theoretical results, the moments of the data do not provide good estimates of actual transport behavior when truncation occurs. This is because the classical moment methods require the full distribution of data, i.e., until the in-stream solute concentration returns to background level. The moments can be more accurately estimated when truncation is explicitly considered [*Luo et al.*, 2006]. However, the proper form of the storage residence time distribution must be chosen to successfully employ the method, and therefore enough data must be obtained to identify the proper residence time distribution. Breakthrough curves with power law tailing reflect hyporheic residence times that are power-

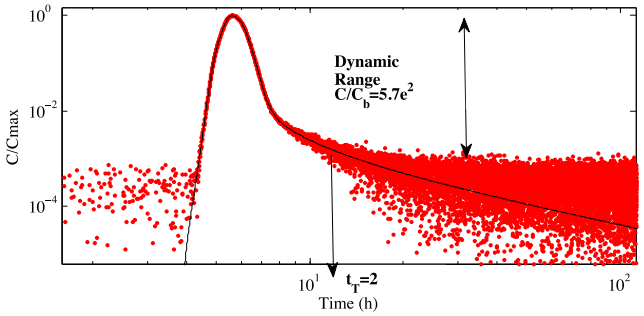

Figure 6. Noise added to a breakthrough curve. The parameters used to generate the continuous time random walk (CTRW) solute breakthrough curve were u = 0.104 m s^{-1}, D = 0.45 m s^{-2}, $\Lambda_1 = 5e^{-5}$ and $\varphi_1 = \exp^{-\frac{1}{500}t}$, $\Lambda_2 = 5e^{-5}$ and $\varphi_2 = t - 1.33$ for a power law distribution. A random noise with a mean of zero and standard deviation of $1e^{-2}$ was added to each data point.

law-distributed with infinite mean [*Haggerty et al.*, 2000]. This implies that some solute is permanently immobilized from the river, for example, in subsurface stagnation zones [*Cardenas*, 2008]. Since solute continues to enter the subsurface from the river, and a portion of that solute will not return to the river during the measurement period, in-stream breakthrough curves will continue to lose mass over time [*Schumer*, 2003].

[15] In order to demonstrate sensitivity truncation, we generated a breakthrough curve with a power law residence time distribution (u = 0.104 m s^{-1}, D = 0.45 m s^{-2}, $\Lambda_1 = 5e^{-5}$ and $\varphi_1 = \exp^{-\frac{1}{500}t}$, $\Lambda_2 = 5e^{-5}$ and $\varphi_2 = t^{-} 1.33$). In order to demonstrate how noise affects tracer breakthrough curve results we added a random noise with a mean of zero and standard deviation of $1e^{-3.5}$ to each normalized model concentration output (C/C_{MAX}) (Figure 6). As the tracer concentration decreased in the tail of the breakthrough curve, the signal-to-noise ratio decreased until the tracer signal could not be reliably distinguished from background. This caused sensitivity truncation at $t_T = 2$. In this case the dynamic range (ratio between the peak value and minimum reliably determined concentration) was $5.7e^2$ (Figure 6). The resolution of the breakthrough curve tail can be improved by increasing the tracer mass injected or increasing the measurement sensitivity. Increasing the injected mass by factors of 10, 30, and 70 increased the truncation time to $t_T = 5$, 10, and 20, and the dynamic range to $3.7e^3$, $1.1e^4$, and $2.9e^4$. A dynamic range of $2.9e^4$ was needed in order to achieve a tail truncation time of 20, the value we previously found to appropriately characterize in-stream breakthrough curves resulting from power law residence time distributions. The dynamic range needed to achieve $t_T = 20$ will differ based on stream conditions, including velocity, dispersion, storage flux, and residence time. The information content of tracer-injection studies can be maximized by choosing a tracer, injected mass, and analytical method in order to achieve the maximum dynamic range for the study. Background concentration and variability cannot be controlled, making it essential to carefully measure background tracer conditions in the stream. By analyzing tracer concentrations upstream of the injection site, it is possible to confirm the minimum tracer value detected reliably above background and therefore the sensitivity truncation time in the breakthrough curve.

4. Discussion

[16] From the synthesis of tracer-injection studies we found that the majority of breakthrough curve tails were truncated due to experimental and/or sensitivity truncation. Tail estimation in sample data subject to truncation is an issue in diverse fields including finance [*Beirlant and Guillou*, 2001], hydrology [*Jawitz*, 2004], signal processing, and sociology [*Nuyts*, 2010]. Both cases of truncation for this review are illustrated in Figure 7. Experimental truncation occurs when sampling is stopped before the form of the storage residence time distribution can be uniquely determined from the tracer data (Figure 7a). The vertical dashed line represents a sampling cut-off time prior to return to background concentrations. The tracer mass that is not measured as a result of this truncation is indicated by the shaded area of the tail. Sensitivity truncation occurs when the dynamic range is not large enough to adequately characterize the form of the storage residence time distribution (Figures 7b and 7c). The two main cases of sensitivity truncation are due to an analytical method sensitivity limit, i.e., when the tracer background concentration is below the limit of detection of the instrument, as shown in Figure 7b, or due to high variability in tracer background concentrations as shown in Figure 7c. In these cases, only the tracer concentrations above the sensitivity limits are detected, as indicated by the area shaded in gray under the peak of the breakthrough curve in Figures 7b and 7c. The unmeasured mass in the tail of the breakthrough curve due to truncation leads to an underestimation of the residence times of solute in storage and thus an overestimation of the biogeochemical processes that occur when a reactive solute is transported and reacted within storage areas.

[17] For many tracers, there may be considerable background concentration that may vary over time due to a combination of flow fluctuations and variable inputs into the stream. The background variability of tracer impacts the estimation of transport parameters [*Field*, 2011]. In order to characterize background variability, measurements or samples should be taken before and throughout the experiment, upstream of the injection site. In cases where experimental stream reaches are long, or the conditions at the upstream and downstream sampling locations are different, this approach may not work. For this reason, it is also advisable to measure background concentrations for a day or so before and after the experiment at the given sampling location. This approach will provide a good sense of variability in background concentrations. Then by comparing these values to the tracer concentration values, particularly in the tail, it will be clear when the tracer concentration cannot be distinguished from the background. Determining the dynamic range is especially important when the breakthrough curve has power law tailing with a logarithmic decrease to the background. Therefore, it is important to measure the breakthrough curve for a sufficiently long time until the appropriate residence time distribution can be chosen to represent stream storage. Experiments should be designed to maximize dynamic range in order to characterize the widest possible range of residence times. Experiment designs that do not consider the possibility of long residence

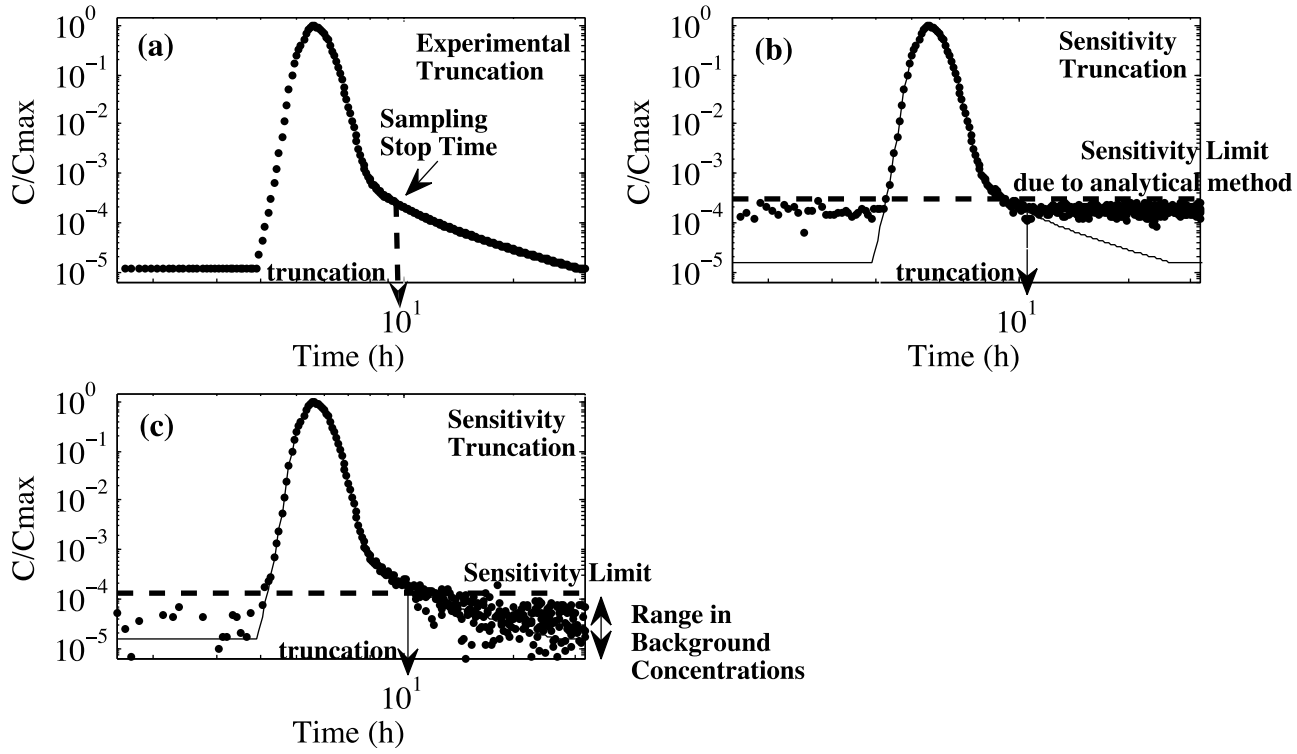

Figure 7. Illustrations of experimental and sensitivity truncation. (a) Experimental truncation resulting from cessation of sampling before the form of the breakthrough curve can be determined. (b) Sensitivity truncation resulting from an analytical sensitivity limit (limit of detection). (c) Sensitivity truncation resulting from high background variability.

time distributions will artificially limit the range of transport timescales that can be characterized, leading to incorrect estimates of both transport and reaction parameters in cases where the underlying transport behavior shows power-law storage behavior.

[18] Several methods can be used to increase the dynamic range. The maximum possible tracer mass should be injected. This is typically limited by factors such as cost, solubility limits in the injectate solution, potential acute toxicity of the tracer to aquatic fauna, and the need to avoid producing significant density differences between the injectate and the stream. Higher-sensitivity tracers and ones with low or nil natural background should be preferred. Most notably, tritium and fluorescent tracers provide much higher dynamic range than salts. Further, it is always important to account for analytical error, detection limits, and background tracer variability. In addition to adequately measuring the tracer background concentrations, analytical error can be accounted for with repeat measurements of a sample with known tracer concentration to determine the noise inherent in the method. Here it is not sufficient to determine analytical error only on laboratory standards. Because of the potential for background variability and interferences between natural water constituents and analytical methods, standard-additions should be performed using stream water to determine effective analytical noise and detection levels under field conditions. These precautions should be applied to sensors deployed in situ as well as grab samples analyzed in laboratory settings. It should also be noted that dynamic range decreases from upstream to downstream sampling stations as the injected tracer mass becomes diluted during downstream transport.

[19] Sampling of the subsurface and surface storage area can enhance the injection study results by providing information on the solute residence time distribution in these regions. The observations of tritium concentration in pore water shown in Figure 4 were needed to confirm the optimal model choice for analysis of the surface breakthrough curve. The subsurface data would have been even more important with further truncation of the in-stream breakthrough curve, as was observed in the same tracer-injection study at downstream sampling sites. Storage increased due to the incorporation of more hyporheic transport paths with downstream solute transport, which increased the error in the storage parameters with distance downstream due to truncation and insufficient mass-recovery [*Wörman and Wachniew*, 2007].

[20] It is important to collect sufficient data to choose the form of storage residence time distribution that will appropriately characterize the stream and its storage properties. Similarly, it is important to consider if truncation has occurred when choosing the model that will be used to estimate stream transport parameters. Rates and timescales of storage inferred from fitting breakthrough curves are strongly influenced by observation time and sensitivity. Choosing a tracer with high sensitivity and ensuring high dynamic range for detection of the tracer above background noise levels is essential to adequately characterize transport and tailing behavior. Another issue to consider is sampling at a far enough distance downstream in order to achieve full mixing throughout the channel cross-section, meaning the

dispersion coefficient is stationary. A theoretical study showed that the mixing length required to reach asymptotic dispersion was 150 stream widths [*Wang et al.*, 2012]. Incomplete mixing over the cross-section also produces skewed breakthrough curves and nonlinear growth of the variance [*Fischer et al.*, 1979]. This occurs because solute within either quicker or slower transport paths remains on those separate paths due to incomplete mixing, enhancing the variance of the observations.

[21] We found that a truncation time of $t_T = 20$ was sufficient to characterize power law tailing in breakthrough curves. However, the appropriate truncation time may vary based on the storage properties of the stream influenced by the sediment bed characteristics or geomorphic controls on solute transport. Even when the experiment design yields enough information on tailing behavior, choice of an inappropriate model formulation can lead to significant underestimation of storage timescales. Transient storage models using advection-dispersion and exponential residence time distributions (e.g., OTIS) cannot appropriately account for the full range of residence times often observed in streams (Figure 5), leading to substantial underestimates of both in-stream dispersion and hyporheic storage times in systems that show extended residence time distributions. The only way to adequately determine when the residence time distributions are actually thin (i.e., exponential) or heavy-tailed (i.e., power law) is to track in-stream concentrations down to the true background or to obtain complementary observations of solute retention in storage zones. When analytical error or background variability preclude determination of the long-term tailing behavior, then it is essential that the truncation time be reported, as this represents the longest timescale of transport that is adequately characterized by the available data. A review of groundwater tracer studies also found that information needed for a mass transfer model is lost due to truncation [*Haggerty et al.*, 2004]. Particularly, groundwater transport characterization was subject to error at timescales longer than the experimental duration and model fits were dependent on the experimental conditions.

[22] As demonstrated with experimental data and model simulations of commonly observed in-stream breakthrough curves, tail truncation leads to considerable underestimation of solute residence times. This leads to the incorrect conclusion that there is relatively quick turnover of the solute between surface water and the hyporheic zone that limits the amount of biogeochemical reactions that may take place. Without choosing the appropriate form of residence time distribution, the inverse modeling of breakthrough curves will not accurately characterize stream transport and retention. A more flexible model (e.g., CTRW or MRMT) can help avoid having the model formulation artificially limit the range of storage timescales. Improved fitting methods can also be used to better estimate tail parameters [*Nuyts*, 2010]. If truncation is known to occur then it can be accounted for as long as the residence time distribution is appropriately chosen and parameter estimates are constrained using the data available [*Luo et al.*, 2006]. Even with a power law distribution of solute in storage, eventually the breakthrough curve will temper to an exponential decay due to the natural cut-off time when asymptotic conditions are reached and the anomalous solute transport behavior transitions to Gaussian. Thus, a power law residence time distribution without tempering will slightly overestimate the solute residence times in storage. A model that incorporates this tempered behavior has been developed and can be applied if the natural cut-off timing is known [*Dentz et al.*, 2004; *Meerschaert et al.*, 2008]. However, in the tracer injection studies reviewed here experimental or sensitivity truncation occurred before the natural cut-off and tempering of the breakthrough curve was observed. Alternatively, non-parametric methods have recently been used to derive stream transport parameters without choosing a model or storage residence time distribution that artificially truncates the breakthrough curve tail [*Gooseff et al.*, 2011].

[23] Based on the results presented here, we recommend the following improvements to the design of tracer-injection experiments:

[24] 1) Characterize the variability of tracer background concentrations with periodic in-stream tracer measurements upstream of the injection location before, during, and after the experiment. For longer-term experiments measure diel variation of tracer background concentrations.

[25] 2) Rigorously evaluate the error and detection limit of the analytical method in order to differentiate between background variability and instrument error.

[26] 3) Sample at each downstream sampling site for at least 20 times the mean in-stream travel time after the injection has ended.

[27] 4) Inject enough tracer mass to achieve a dynamic range that will not truncate the tail until at least 20 times the mean travel time after the injection has ended. For example, a dynamic range of $2.9e^4$ is needed to characterize a breakthrough curve with a power law slope of 1.33.

[28] 5) Statistically evaluate the uncertainty and uniqueness of model fits.

[29] 6) Report how all transport properties, including stream velocity and dispersion coefficients were determined, and the uncertainty in each measurement.

[30] **Acknowledgments.** The authors would like to thank B. Cardenas, R. Haggerty, and one anonymous reviewer for helpful comments on an early version of this paper. The project was funded by NSF grants EAR-0810270 and DEB-0543442, by the Water Cycle Dynamics in a Changing Environment hydrologic synthesis project (NSF EAR 06-36043) led by M. Sivapalan at the University of Illinois, and by an Environmental Protection Agency (EPA) STAR Fellowship awarded to J. Drummond. R. Schumer was partially supported by the National Center for Earth Surface Dyanmics, an NSF Science and Technology Center funded under agreement EAR-0120904. We thank J. Tank for her guidance as a session mentor and M. Hassan for coordinating the summer institute at the University of British Columbia. We would also like to thank K. Simonson, A. Salus, and B. Gibbons for their assistance in the meta-data analysis and all the collaborators who provided data to the summer institute. This project was developed by T. Covino and J. Drummond at the hydrologic synthesis summer institute with support from D. Leong and S. Patil. The CTRW model and fitting analysis was developed by A. F. Aubeneau. A. Packman and R. Schumer provided input and guidance as session mentors.

References

Alexander, R. B., J. K. Böhlke, E. W. Boyer, M. B. David, J. W. Harvey, P. J. Mulholland, S. P. Seitzinger, C. R. Tobias, C. Tonitto, and W. M. Wollheim (2009), Dynamic modeling of nitrogen losses in river networks unravels the coupled effects of hydrological and biogeochemical processes, *Biogeochemistry*, *93*, 91–116, doi:10.1007/s10533-008-9274-8.

Argerich, A., E. Martí, F. Sabeter, M. Ribot, D. von Schiller, and J. L. Riera (2008), Combined effects of leaf litter inputs and a flood on nutrient retention in a Mediterranean mountain stream during fall, *Limnol. Oceanogr.*, *53*(2), 631–641, doi:10.4319/lo.2008.53.2.0631.

Battin, T. J., L. A. Kaplan, S. Findlay, C. S. Hopkinson, E. Martí, A. I. Packman, J. D. Newbold, and F. Sabater (2008), Biophysical

controls on organic carbon fluxes in fluvial networks, *Nat. Geosci.*, *1*, 95–100, doi:10.1038/ngeo101.

Beirlant, J., and A. Guillou (2001), Pareto index estimation under moderate right censoring, *Scand. Actuar. J.*, *2001*(2), 111–125, doi:10.1080/03461230152592764.

Bencala, K. E., and R. A. Walters (1983), Simulation of solute transport in a mountain pool-and-riffle stream: A transient storage model, *Water Resour. Res.*, *19*(3), 718–724, doi:10.1029/WR019i003p00718.

Berkowitz, B., A. Cortis, M. Dentz, and H. Scher (2006), Modeling non-fickian transport in geological formations as a continuous time random walk, *Rev. Geophys.*, *44*, RG2003, doi:10.1029/2005RG000178.

Boano, F., A. I. Packman, A. Cortis, R. Revelli, and L. Ridolfi (2007), A continuous time random walk approach to the stream transport of solutes, *Water Resour. Res.*, *43*(10), W10425, doi:10.1029/2007WR006062.

Cardenas, M. B. (2007), Potential contribution of topography-driven regional groundwater flow to fractal stream chemistry: Residence time distribution analysis of Tóth flow, *Geophys. Res. Lett.*, *34*, L05403, doi:10.1029/2006GL029126.

Cardenas, M. B. (2008), Surface water-groundwater interface geomorphology leads to scaling of residence times, *Geophys. Res. Lett.*, *35*, L08402, doi:10.1029/2008GL033753.

Choi, J., J. W. Harvey, and M. H. Conklin (2000), Characterizing multiple timescales of stream and storage zone interaction that affect solute fate and transport in streams, *Water Resour. Res.*, *36*(6), 1511–1518, doi:10.1029/2000WR900051.

Cortis, A., and B. Berkowitz (2005), Computing 'anomalous' contaminant transport in porous media: The CTRW MATLAB tool- box, *Ground Water*, *43*(6), 947–950, doi:10.1111/j.1745-6584.2005.00045.x.

Dentz, M., A. Cortis, H. Scher, and B. Berkowitz (2004), Time behavior of solute transport in heterogeneous media: Transition from anomalous to normal transport, *Adv. Water Resour.*, *27*, 155–173, doi:10.1016/j.advwatres.2003.11.002.

Field, M. S. (2011), Application of robust statistical methods to background tracer data characterized by outliers and left-censored data, *Water Res.*, *45*(10), 3107–3118, doi:10.1016/j.watres.2011.03.018.

Fischer, H. B., E. J. List, and R. C. Y. Koh, J. lmberger, and N. H. Brooks (1979), *Mixing in Inland and Coastal Waters*, Academic, San Diego, Calif.

Gooseff, M. N., S. M. Wondzell, R. Haggerty, and J. Anderson (2003), Comparing transient storage modeling and residence time distribution (RTD) analysis in geomorphically varied reaches in the Lookout Creek basin, Oregon, USA, *Adv. Water Resour.*, *26*, 925–937, doi:10.1016/S0309-1708(03)00105-2.

Gooseff, M. N., J. LaNier, R. Haggerty, and K. Kokkeler (2005), Determining in-channel (dead zone) transient storage by comparing solute transport in a bedrock channel-alluvial channel sequence, Oregon, *Water Resour. Res.*, *41*, W06014, doi:10.1029/2004WR003513.

Gooseff, M. N., D. A. Benson, M. A. Briggs, M. Weaver, W. Wollheim, B. Peterson, and C. S. Hopkinson (2011), Residence time distributions in surface transient storage zones in streams: Estimation via signal deconvolution, *Water Resour. Res.*, *47*, W05509, doi:10.1029/2010WR009959.

Haggerty, R., and S. M. Gorelick (1995), Multiple-rate mass transfer for modeling diffusion and surface reactions in media with pore-scale heterogeneity, *Water Resour. Res.*, *31*(10), 2383–2400, doi:10.1029/95WR10583.

Haggerty, R., S. A. McKenna, and L. C. Meigs (2000), On the late-time behavior of tracer test breakthrough curves, *Water Resour. Res.*, *36*(12), 3467–3479, doi:10.1029/2000WR900214.

Haggerty, R., S. M. Wondzell, and M. A. Johnson (2002), Power-law residence time distribution in the hyporheic zone of a 2nd-order mountain stream, *Geophys. Res. Lett.*, *29*(13), 1640, doi:10.1029/2002GL014743.

Haggerty, R., C. F. Harvey, C. Freiherr von Schwerin, and L. C. Meigs (2004), What controls the apparent timescale of solute mass transfer in aquifers and soils? A comparison of experimental results, *Water Resour. Res.*, *40*, W01510, doi:10.1029/2002WR001716.

Harvey, J. W., and B. J. Wagner (2000), Quantifying hydrologic interactions between streams and their subsurface hyporheic zones, in *Streams and Groundwaters*, edited by J. B. Jones and P. J. Mulholland, pp. 3–44, Academic, San Diego, Calif., doi:10.1016/B978-012389845-6/50002-8.

Jawitz, J. W. (2004), Moments of truncated continuous univariate distributions, *Adv. Water Resour.*, *27*(3), 269–281, doi:10.1016/j.advwatres.2003.12.002.

Johansson, H., K. Jonsson, K. J. Forsman, and A. Wörman (2001), Retention of conservative and sorptive solutes in streams - Simultaneous tracer experiments, *Sci. Total Environ.*, *266*, 229–238.

Luo, J., O. A. Cirpka, and P. K. Kitanidis (2006), Temporal-moment matching for truncated breakthrough curves for step or step-pulse injection, *Adv. Water Resour.*, *29*, 1306–1313.

Marion, A., M. Zaramella, and A. Bottacin-Busolin (2008), Solute transport in rivers with multiple storage zones: The STIR model, *Water Resour. Res.*, *44*, W10406, doi:10.1029/2008WR007037.

McGuire, K. J., and J. J. McDonnell (2006), A review and evaluation of catchment transit time modeling, *J. Hydrol.*, *330*, 543–563, doi:10.1016/j.jhydrol.2006.04.020.

Meerschaert, M. M., Y. Zhang, and B. Baeumer (2008), Tempered anomalous diffusion in heterogeneous systems, *Geophys. Res. Lett.*, *35*, L17403, doi:10.1029/2008GL034899.

Nuyts, J. (2010), Inference about the tail of a distribution: Improvement on the Hill estimator, *Int. J. Math. Math. Sci.*, *2010*, 924013, doi:10.1155/2010/924013.

Payn, R. A., M. N. Gooseff, B. L. McGlynn, K. E. Bencala, and S. M. Wondzell (2009), Channel water balance and exchange with subsurface flow along a mountain headwater stream in Montana, United States, *Water Resour. Res.*, *45*, W11427, doi:10.1029/2008WR007644.

Peterson, B. J., et al. (2001), Control of Nitrogen Export from Watersheds by Headwater Streams, *Science*, *292*(5514), 86–90, doi:10.1126/science.1056874.

Schumer, R., D. A. Benson, M. M. Meerschaert, and B. Baeumer (2003), Fractal mobile/immobile solute transport, *Water Resour. Res.*, *39*(10), 1296, doi:10.1029/2003WR002141.

Schumer, R., M. M. Meerschaert, and B. Baeumer (2009), Fractional advection-dispersion equations for modeling transport at the Earth surface, *J. Geophys. Res.*, *114*, F00A07, doi:10.1029/2008JF001246.

Triska, F. J., V. C. Kennedy, R. J. Avanzino, G. W. Zellweger, and K. E. Bencala (1989), Retention and transport of nutrients in a third-order stream: Channel processes, *Ecology*, *70*(6), 1877–1892, doi:10.2307/1938119.

Wang, L., M. B. Cardenas, W. Deng, and P. C. Bennett (2012), Theory for dynamic longitudinal dispersion in fractures and rivers with Poiseuille flow, *Geophys. Res. Lett.*, *39*, L05401, doi:10.1029/2011GL050831.

Workshop, S. S. (1990), Concepts and methods for assessing solute dynamics in stream ecosystems, *J. N. Am. Benthol. Soc.*, *9*, 95–119, doi:10.2307/1467445.

Wörman, A., and P. Wachniew (2007), Reach scale and evaluation methods as limitations for transient storage properties in streams and rivers, *Water Resour. Res.*, *43*, W10405, doi:10.1029/2006WR005808.

Wörman, A., A. I. Packman, H. Johansson, and K. Jonsson (2002), Effect of flow-induced exchange in hyporheic zones on longitudinal transport of solutes in streams and rivers, *Water Resour. Res.*, *38*(1), 1001, doi:10.1029/2001WR000769.

Zarnetske, J. P., R. Haggerty, S. M. Wondzell, and M. A. Baker (2011), Dynamics of nitrate production and removal as a function of residence time in the hyporheic zone, *J. Geophys. Res.*, *116*, G01025, doi:10.1029/2010JG001356.